Euro-Mediterranean Journal for Environmental Integration
https://doi.org/10.1007/s41207-024-00463-w

CONFERENCE PAPER

Modified hemp fibers as a novel and green adsorbent for organic dye adsorption: adsorption, kinetic studies and modeling

Gianluca Viscusi[1] · **Francesco Napolitano**[1] · **Giuliana Gorrasi**[1]

Received: 12 September 2023 / Accepted: 10 January 2024

Abstract

Synthetic dyes represent a serious hazard to aquatic environments. Many approaches for eliminating these contaminants have been devised and applied. This manuscript reports the production of a novel, low-cost and ecologically friendly bioadsorbent based on hemp fibers that are functionalized with graphite oxide through bridging with an organosilane. Methylene blue was selected as a typical pollutant to be removed from wastewaters. The adsorbent was characterized through scanning electron microscopy (SEM), energy-dispersive X-ray spectroscopy (EDX) and Fourier-transform infrared (FTIR) analysis. An investigation of the effects of pH and temperature on the adsorption process was carried out. The adsorption capacity increased with increasing contact time as well as with the temperature, proving that the process shows endothermic behavior. Moreover, the process was found to be dependent on the pH level and, to corroborate the collected results, the point of zero charge was evaluated. The maximum adsorption capacity was found to be 57 mg/g, which was achieved with the following parameters: pH = 7.5, T = 80 °C and an initial dye concentration equal to 5 mg/L. Reusability studies showed a 15% decrease in adsorption capacity after 30 adsorption tests, proving the possibility of reusing the produced adsorbent without any great decay in performance. Finally, a potential adsorption mechanism is reported and discussed. The reported results prove that it is feasible to apply the designed adsorbent of organic dyes to the purification of wastewaters.

Graphical abstract

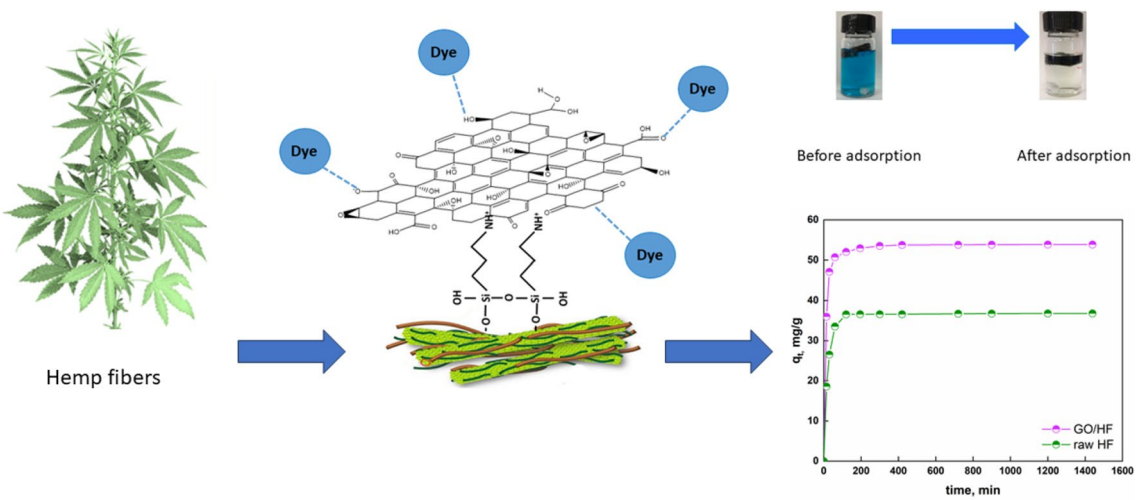

Keywords Hemp fiber · Water purification · Graphite oxide · Natural fiber · Adsorption · Advanced materials

Responsible Editor: Mohamed Ksibi.

Extended author information available on the last page of the article

Published online: 05 March 2024

Introduction

Water is essential for the survival of life, but it has been polluted by dyes and fertilizer and through anthropogenic activities (Zafar et al. 2021), the depletion of crude oil resources (Sehar et al. 2020), rapid urbanization, individual mobility, increasing energy demands (Yin et al. 2020; Al-Rawi et al. 2020; Faridi et al. 2023), and incomplete combustion, which affects human health and the ecosystem (Rasheed et al. 2021). The presence of organic pollutants in the aquatic environment, which can cause adverse biological impacts, is leading to great concern over ecosystems. For example, traces of synthetic dyes in wastewaters represent a major issue due to their impact on ecosystems and their effect on the health of people (Tkaczyk et al. 2020; Viscusi et al. 2021a; Ma et al. 2022). Dyes are now used in different industrial fields, such as the textile industry, paper production, food technology, photochemical cells, agricultural research and hair coloring (Crini et al. 2019; Molla and Youk 2022; Shi et al. 2022). Different methodologies have been applied to remove pollutants, such as solvent extraction, flocculation, chemical oxidation, coagulation and adsorption (Hao et al. 2000; Forgacs et al. 2004; Zhang et al. 2016; Thong et al. 2018; Varghese et al. 2019; Kong and Wilson 2020), microbial fuel cells (Mohyudin et al. 2022), and catalysis (Al-Rawi et al. 2021). Adsorption is considered the methodology most commonly used to remove organic dyes, since this technology is quite simple and cheap (Wang et al. 2020; Viscusi et al. 2021b; Sağlam et al. 2023). Moreover, the use of common adsorbents can make the adsorption process quite expensive (Viscusi et al. 2022). So, the scientific community is focusing on the use of novel and sustainable low-cost adsorbents (Kong and Wilson 2020; Abbaz et al. 2023). Different natural materials have been used to remove pollutants from wastewaters, such as apricot seed shell (Hashem et al. 2022), aloe vera leaf waste (Khaniabadi et al. 2016), kapok fibers (Futalan et al. 2022), modified cotton fibers (Yang et al. 2022), almond peel waste (Al-Musawi et al. 2023), pineapple peels (Widiartyasari Prihatdini et al. 2023), orange peels (Eddy et al. 2023), date seed (Ali et al. 2017), clam shell (Qu et al. 2022), sesame hull (Feng et al. 2011), pomegranate peels (Abbaz et al. 2023), sugarcane bagasse ash (Garg et al. 2023) and an algae-based composite (Smječanin et al. 2022). One of the most interesting types of agro-waste materials is natural fibers. These materials are emerging mainly due to their advantageous properties such as low cost, availability and biodegradability (Faruk et al. 2012; Liu et al. 2017; Sanjay et al. 2019; Viscusi et al. 2020, 2021d). Among natural fibers, hemp fibers (*Cannabis sativa* L.) are attracting the interest of the scientific community because of their features: thermal insulation, low cost, no irritation, and a rapid growing cycle (Morin-Crini et al. 2018; Viscusi et al. 2020, 2021c; Viscusi and Gorrasi 2021). However, hemp fibers cannot be used as a highly effective adsorbent without modifying or treating them. So, this work proposes a sustainable approach to improve the adsorption properties of hemp fibers by modifying them with graphite oxide through chemical modification with a common organosilane, 3-aminopropyl triethoxysilane (OS). The use of carbon and carbon-derived materials for wastewater remediation has been widely explored. Sher et al. applied an electrochemical technique in combination with powdered activated carbon for the removal of micropollutants by adsorption (Sher et al. 2021). Rashtbari et al. developed zerovalent iron nanoparticles incorporated on activated carbon from pomegranate peel extract as an efficient and inexpensive adsorbent to eliminate furfural (Rashtbari et al. 2022). Moreover, different carbon-based materials have been used for water remediation, such as activated carbon (Rosli et al. 2023), graphene oxide (Konicki et al. 2017), reduced graphene oxide (Gupta and Khatri 2017), multi-walled carbon nanotubes (MWCNTs) (Shirmardi et al. 2013), mesoporous carbon materials (Mohammadi et al. 2011) and biochar materials (Ouedrhiri et al. 2022). Notwithstanding, up to now, despite the wide use of carbon for adsorption processes, there have not been any deep studies of novel adsorbents based on hemp fibers modified with graphene oxide. To study the adsorption capacity of the adsorbent designed in the present work, batch adsorption studies were carried out to evaluate the sorption of methylene blue. The effects of temperature and pH on the adsorption performance were then considered. Finally, reusability studies were carried out. Since the use of a powder-form adsorbent can generate pollution, separation and regeneration processes are needed to limit the use of these materials. It follows that the use of hemp fiberboard will allow the easy handling of the adsorbent, facilitating desorption and reusability processes and thus limiting operating costs.

Experimental

Materials

Hemp fibers (HF) were provided by Nafco Company. The organosilane [3-aminopropyl)triethoxysilane (OS)] and NaOH in pellet form were purchased from Sigma–Aldrich, while HCl solution 37% v/v and NaCl were purchased from Carlo Erba Reagents. Graphite oxide was received from Qingdao Tianhe Graphite Co. Ltd. Methylene blue was purchased from Panreac AppliChem ITW Reagents.

Surface modification

OS (5% wt) was hydrolyzed in water at 50 °C for 2.5 h (pH = 3). After removing impurities, the HFs were modified with OS solution (T = 25 °C; solid/liquid ratio equal to 0.03 g/mL) for 1.5 h. Due to the self-condensation of OS, siloxane oligomers with Si–OH groups can be formed (Raji et al. 2016). They are able to form hydrogen bonds with the hydroxyl groups of the HF (Kale et al. 2019). Graphite oxide (GO) in aqueous solution (0.2% w/w) was prepared by dissolving GO in water and using ultrasonication to make the dispersion homogeneous. The silane-modified HFs were soaked in the GO/water mixture for 48 h at 90 °C. Finally, the HF/GO samples were dried in an oven at 150 °C for 24 h. The functionalization of GO with OS-modified HF is based on either the reaction of the OH groups of GO with the Si–OH groups through the formation of Si–O–C bonds or the reaction of epoxy groups with the amino groups of the OS, leading to the formation of secondary amines (Li et al. 2016; Serodre et al. 2019). After that, the modified HF were washed and dried.

Methods

Scanning electron microscopy (SEM) was used to study the material's morphology. A Quanta 200 F microscope was used to acquire SEM images. Before the analysis, the samples were coated with a thin film of gold through sputtering.

Fourier transform infrared (FTIR) analysis was performed using a Bruker spectrometer (model Vertex 70; average of 64 scans, resolution of 4 cm^{-1}). This technique allows the changes and shifts in functional groups due to functionalization to be evaluated. The specimens were ground in KBr powder before they were dried under vacuum at room temperature.

Each spectrum was recorded 64 times with a resolution of 4 cm^{-1}. The blank spectrum was recorded under the same conditions by using a pure KBr sample.

The point of zero charge (pH_{PZC}) was evaluated by adopting a titration-based procedure (Viscusi et al. 2021a). A set amount of adsorbent was added to the NaCl solution to achieve equilibration before drops of HCl solution were added for titration. The pH was analyzed and ΔpH (final pH − initial pH) was plotted. The point where the curve intersected the x axis was identified as pH_{pzc}.

By monitoring volumetric N_2 adsorption on the samples at – 196 °C with the Costech Sorptometer 1042 analyzer, the specific surface area values of the samples were determined.

Batch adsorption tests were carried out as follows. Methylene blue (MB) solutions were prepared in distilled water (5 mg/L). The pH of the MB solution was varied (from 3 to 12) by adding drops of NaOH or HCl solution (1 M). The concentration of MB in the solution was evaluated using the UV–Vis technique (absorbance at λ = 664 nm). The adsorption capacity (q_t) was evaluated through Eq. 1:

$$q_t = \frac{(c_0 - c_{eq}) \times V}{m}, \tag{1}$$

where c_0 is the initial dye concentration, c_{eq} is the equilibrium dye concentration, V is the volume of the solution and m is the mass of the membrane (Mohammad and Atassi 2020). Various kinetic models have been used to model adsorption data, such as Lagergren's pseudo-first-order model (Eq. 2), a pseudo-second-order model (Eq. 3) an intra-particle diffusion model (Eq. 4) (Slatni et al. 2022) and Elovich's model (Eq. 5) (Zhou et al. 2014; Largitte and Pasquier 2016):

$$\log\left(q_e - q_t\right) = \log\left(q_e\right) - \frac{k_1}{2.303} \times t \tag{2}$$

$$\frac{t}{q_t} = \frac{1}{k_2 \times q_e^2} + \frac{t}{q_e} \tag{3}$$

$$q_t = k_{id} \times \sqrt{t} + C \tag{4}$$

$$q_t = \frac{1}{\beta} \ln(\alpha\beta) + \frac{1}{\beta} \ln\left(t + t_0\right), \tag{5}$$

where k_1 (1/min) and k_2 (mg/g min) are the rate constants of the first- and second-order models, respectively; q_e (mg/g) is the equilibrium amount of dye adsorbed per gram of adsorbent; C is the intercept of the intraparticle diffusion model, k_{id} is the intraparticle diffusion constant; α (mg/g min) is the initial adsorption rate; and β (g/mg) is related to the surface coverage and the activation energy. Desorption studies were then performed by washing the used HF/GO adsorbent with ethanol. The adsorbent was then dried and reused for further adsorption tests.

Computational work

Computation analysis was performed using Materials Studio 8.0 software. The structures of GO and MB were geometrically optimized using the Dmol3 module. The GO–dye system was analyzed using the Amorphous Cell option and optimized using the Forcite module (Task = Geometry Optimization; Forcefield = COMPASS).

Results and discussion

Morphological and spectroscopic analyses

Fig. 1 shows the SEM images of (a) untreated HF and (b) graphite-oxide-functionalized HF.

The SEM image of pristine hemp fibers showed the typical roughened surfaces of natural fibers. Even after being modified with graphite oxide, the hemp fiber surface preserved its morphology. The EDX maps confirmed the atomic weight distribution of Si and N due to organosilane grafting. Figure 1c reports the FTIR spectra of GO, HF and GO/HF. The peak located at about 3400 cm^{-1} is related to OH groups of polysaccharides (Terpáková et al. 2012; Khanjanzadeh et al. 2018). The peaks at about 2910 cm^{-1} and 1736 cm^{-1} concern CH stretching (Agarwal et al. 2010; Terpáková et al. 2012) and C=O stretching (Rachini et al. 2009) vibrations, while the peaks at 1454, 1373, 1314 and 1254 cm^{-1} can be related to CH_2 bending, OH bending of carboxylic acids, C–O groups of polysaccharides and C–O stretching of acetyl groups (Sawpan et al. 2011; Kargarzadeh et al. 2015). The peaks in the range 1162–1030 cm^{-1} concern C–O stretching and C–H rocking vibrations of the pyranose ring skeleton (Kargarzadeh et al. 2012). The OS modification provided new peaks: an N–H bending vibration at 1550 cm^{-1} (Robles et al. 2015; Khanjanzadeh et al. 2018); Si–O–Si and Si–O–C peaks at about 1135 and 1150 cm^{-1}, respectively; and Si–O–C and Si–O stretching vibrations and Si–H bond vibrations at 1040 cm^{-1}, 471 cm^{-1} and 780 cm^{-1}, respectively (Allahbakhsh et al. 2017; Maleki and Karimi-Jashni 2020). In the GO spectrum, the peaks at 2927 and 2868 cm^{-1} are associated with OH groups (Szabó et al. 2005; Jeong et al. 2009; Yan et al. 2017). The C=O carbonyl stretching at 1728 cm^{-1} and the C–O epoxide group stretching at 1229, 1061 and 1036 cm^{-1} are also observed in the FTIR spectrum of modified HF (Loryuenyong et al. 2013; Javed and Hussain 2015; Chong et al. 2018). Finally, the peak at 1625 cm^{-1} is associated with the sp^2 character of C=C groups (Chong et al. 2018).

Kinetic studies

Adsorption capacities of GO/HF and HF

Before evaluating the effects of some experimental parameters on the adsorption capacity of modified HF, raw HF and GO-modified HF were tested to estimate their adsorption capacities. The initial MB concentration was set at 5 mg/l ($T = 20$ °C and pH = 7.5). Adsorption curves are reported in Fig. 2.

The amount of GO on the HF surface was evaluated through gravimetric analysis. The measurements provided a value of 62 ± 2 mg GO/g HF. According to the profiles reported in Fig. 2, GO modification increased the MB

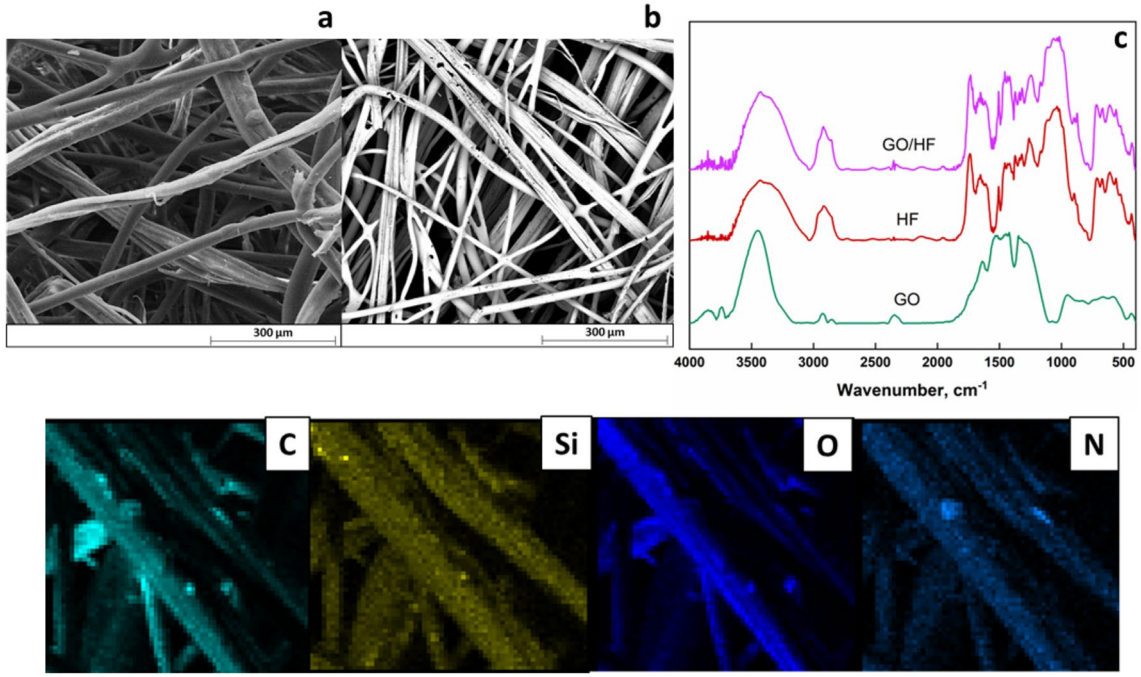

Fig. 1 *Top*: SEM micrographs of **a** HF and **b** GO-functionalized HF. **c** FTIR spectra. *Bottom*: energy-dispersive X-ray spectroscopy (EDX) maps of GO-functionalized HF

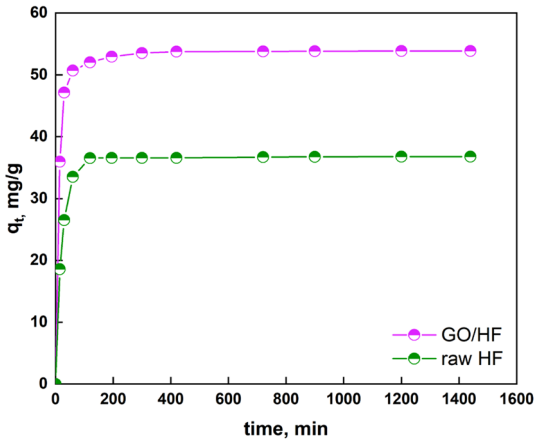

Fig. 2 q_t versus t for the adsorption of MB on raw hemp fibers and GO/HF

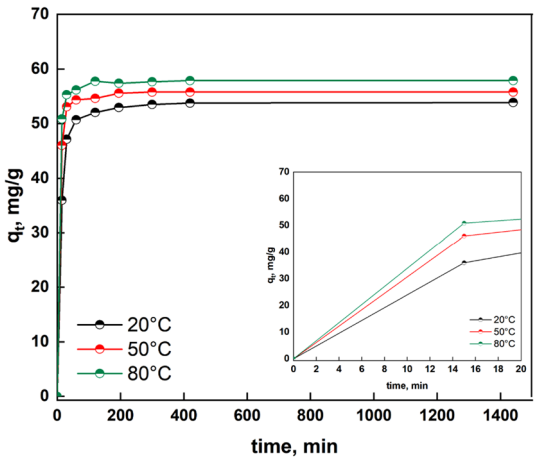

Fig. 3 Adsorption capacity of GO/HF evaluated at pH = 7.5 and T = 20 °C, 50 °C and 80 °C

adsorption capacity of HF from 36.7 mg/g for raw HF to 53.86 mg/g for GO/HF: an increase of roughly 32%. The noticeable enhancement of the adsorption capacity after GO modification is attributed to the increase in specific surface area due to the intrinsically high surface area of GO. The specific surface areas are 45 and 82 m^2/g for raw HF and GO/HF, respectively. These data support the increase in the adsorption capacity after the GO modification.

Effect of temperature

The adsorption kinetics were investigated to better understand the mechanism of adsorption. Figure 3 shows the kinetic curves for adsorbed MB versus contact time (pH = 7.5) obtained at various temperatures (T = 20 °C, 50 °C and 80 °C). The inset shows the adsorption profiles up to 20 min.

The process can be studied by considering two steps:

i) The fast adsorption of MB (t < 20 min) caused by the binding between the cationic dye and the vacant active adsorption sites. For short times, the concentration difference between the liquid and the solid phases is so high that MB adsorption is favored (Kavitha and Namasivayam 2007);
ii) The slow diffusion of the dye molecules due to the fact that adsorption sites have been saturated, before a plateau regime is attained (Li et al. 2013).

As reported in Fig. 3, the adsorption capacity slightly increases upon increasing the temperature, proving the endothermic nature of the adsorption process. As the temperature rises, the rate of diffusion of the dye molecules across the external boundary layer and the internal pores of the adsorbent increases due to the decrease in viscosity (Sajab et al. 2011). Moreover, the increase in temperature affects different parameters such as the free volume, the mobility of the solute, the solubility, the chemical potential of dye molecules (Ho and McKay 1998; Kuang et al. 2020) and the surface activity (Oladipo and Ifebajo 2018). The adsorption data were modeled using the previously reported kinetic models. The fitting curves are depicted in Fig. 4.

The parameters of the kinetic models, as listed in Table 1, were easily evaluated by analyzing the plotted data.

Upon studying the data reported in Table 1, it appears that correlation coefficients were not significant for the pseudo-first-order model. A deviation from the straight line is observed, signifying that this model is not applicable. So, the sorption of methylene blue cannot be considered to be diffusion controlled. Concerning the intraparticle diffusion model, it appears that there could be a mathematical dependence of q_t on the square root of time. As seen in Fig. 4c, the plot of q_t against $t^{1/2}$ gives two straight lines with different slopes and intercepts. The initial linear part of the graph can be attributed to the boundary-layer diffusion of dye molecules, where the adsorption rate is high (Lorenc-Grabowska and Gryglewicz 2007), while the second step concerns the diffusion of dye from the external surface into the pores of the adsorbent followed by adsorption at the active sites of the internal surface. The slope of the linear part is k_{id} and is representative of the rate of the adsorption. Lower values mean a slower adsorption process. Based on the k_{id} values, the rate constants related to the diffusion into pores and adsorption were the highest, showing that the pore diffusion resistance is lower than the diffusion resistance of the boundary layer. Moreover, since the lines have nonzero intercepts (Fig. 4b), it can be claimed that the coexistence of an external film and intraparticle diffusion occurs during the adsorption process (Phuong and Loc 2022).

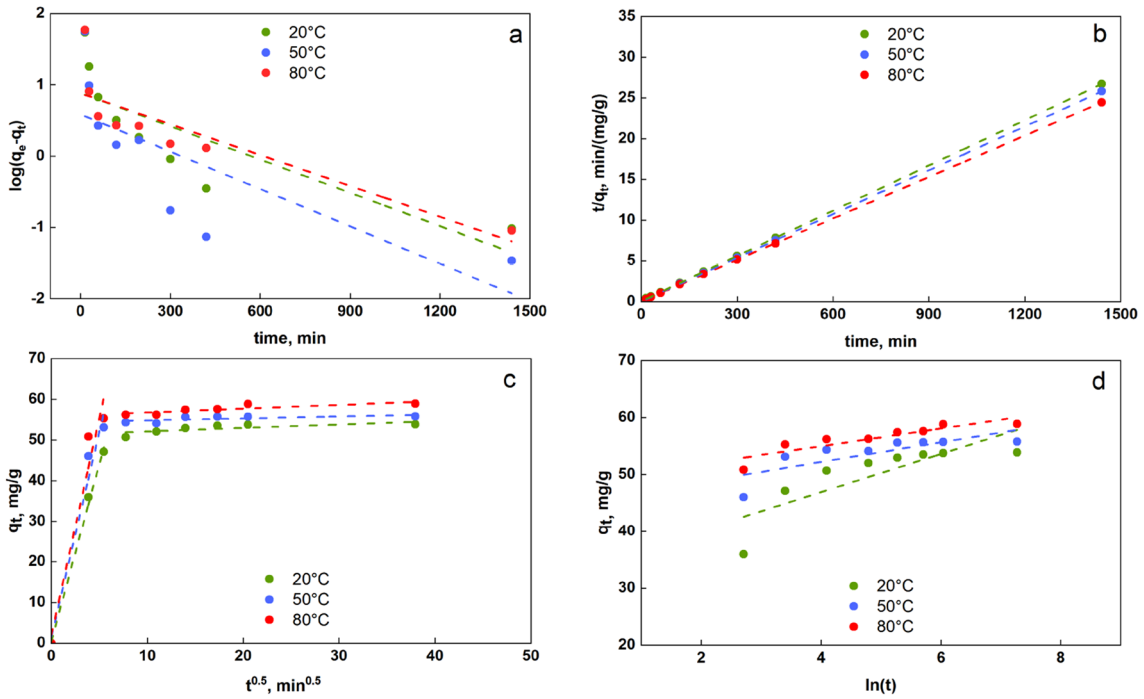

Fig. 4 Comparison of the **a** pseudo-first-order, **b** pseudo-second-order, **c** intra-particle diffusion and **d** Elovich kinetic models for GO/HF at different temperatures (pH = 7.5)

Table 1 Parameters of the kinetic models for MB dye adsorption

	$T = 20$ °C	$T = 50$ °C	$T = 80$ °C
Pseudo-first-order model			
k_1 (1/min)	0.0036	0.040	0.0033
q_e (mg/g)	7.64	3.85	7.58
R^2	0.612	0.504	0.700
Pseudo-second-order model			
q_e (mg/g)	54.05	55.86	59.03
k_2 (mg/g min)	0.0041	0.0092	0.0043
R^2	0.999	0.999	0.999
Intraparticle diffusion step 1			
k_{id} (mg/g $\text{min}^{0.5}$)	8.73	10.09	10.65
C (mg/g)	0.48	1.56	2.17
R^2	0.992	0.945	0.907
Intraparticle diffusion step 2			
k_{id} (mg/g $\text{min}^{0.5}$)	0.086	0.048	0.092
C (mg/g)	51.25	54.35	55.84
R^2	0.45	0.29	0.64
Elovich model			
β (g/mg)	0.29	0.58	0.65
α (mg/g min)	7.5×10^4	4.1×10^{11}	7.3×10^{13}
R^2	0.609	0.543	0.761

Meanwhile, the intercept (C) concerns the boundary layer effect, and it is directly correlated to the mechanism of sorption at the surface in the rate-controlling step (Ahmad et al. 2015). Finally, the adsorption process can be considered to be perfectly modeled by the pseudo-second-order kinetic model ($R^2 > 0.99$), since the calculated adsorption capacities (q_e) were very similar to the experimental ones. Since the best fit was obtained by using pseudo-second-order kinetics, the chemisorption phenomenon can be considered the main diffusion-rate-limiting step among the different interactions between the dye and adsorbent functional groups (Vimonses et al. 2009). The Elovich model was found to fit the experimental data in an unacceptable way considering the resulting low R^2 coefficients.

Mathematical expressions for the constants k_2 and q_e were therefore obtained by interpolating the data reported in the Table 1 as a function of temperature, allowing Eqs. 6 and 7 to be obtained:

$$k_2 = \frac{0.00235}{1 - 0.029 \times T(^{\circ}\text{C}) + 0.0003 \times T^2(^{\circ}\text{C})} \tag{6}$$

$$q_e = 0.083T(^{\circ}\text{C}) + 52.16. \tag{7}$$

Equation 7 indicates that the equilibrium amount of dye sorbed is linearly dependent on T and it is shown to increase as T increases, while a nonlinear dependency of

k_2 on T was observed (Eq. 6). By substituting Eqs. 7 and 6 into Eq. 3, Eq. 8 can be obtained:

$$\frac{t}{q_t} = \frac{425.53 - 12.34 \times T(°C) + 0.127 \times T^2(°C)}{(0.083 \times T(°C) + 52.16)^2} + \frac{t}{0.083 \times T(°C) + 52.16}. \quad (8)$$

The equation reported above allows q_t to be estimated for any contact time at each temperature.

Effect of pH

pH is a fundamental parameter that is known to affect adsorption processes by changing either the surface of the adsorbent or the adsorbate's properties. Figure 5 reports the adsorption capacities of the adsorbent for MB at pH = 3 and pH = 12 at different temperatures.

As T rises, the increased surface activity and kinetic energy of the adsorbate lead to an increase in the removal efficiency (Oladipo and Ifebajo 2018), as previously demonstrated. At low pH, H_3O^+ ions can compete with cationic MB ions, so a reduction in adsorption capacity was observed. Moreover, it is known that the competition between the MB cation and hydrogen ions to form electrostatic interactions with the functional groups of the adsorbent reduces as the pH increases (Shaiful Sajab et al. 2011). Since the point of zero charge (pH_{PZC}) is a key point when investigating the surface charge (Bingol et al. 2010), it was calculated through a titration procedure to deeply study the effect of pH on the adsorption data (Fig. 6).

The pH_{PZC} value is about 6.35. When $pH > pH_{PZC}$, an excess of negative charge is present on the surface adsorbent, which increases the adsorption capacity due to the presence of cationic MB in solution, favoring the formation

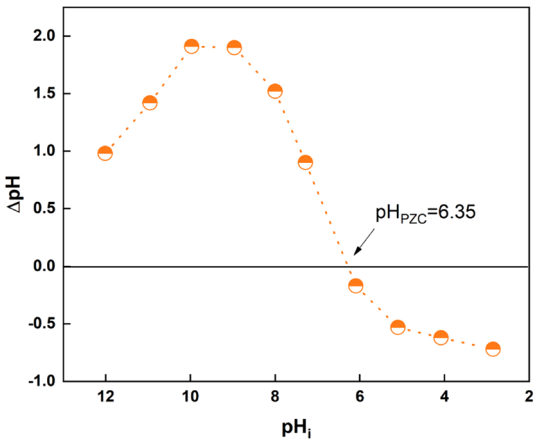

Fig. 6 ΔpH versus pH plot for the evaluation of the point of zero charge

of electrostatic interactions between the oppositely charged groups: the cationic MB and the negative electron-rich sites on the adsorbent surface. When $pH < pH_{PZC}$, an excess of positive charge is present, so repulsive forces should limit the MB adsorption (Li et al. 2020); however, there is still a high adsorption capacity. Focusing on the equilibrium adsorption capacity, Fig. 7 reports the effects of T and pH on the adsorbed dye amount at equilibrium. Figure 7b shows a contour plot of q_e values which clearly shows the dependency of the equilibrium adsorption capacity on the pH and T.

Figure 7 clearly shows the effects of the two investigated parameters on adsorption performance. Temperature seems to have a slight effect on the adsorption capacity, but increasing it leads to higher q_e values, demonstrating the endothermic nature of the process. The effect of pH seems to be nonlinear. At low pH values, repulsive forces are responsible for decreasing the q_e value, as previously

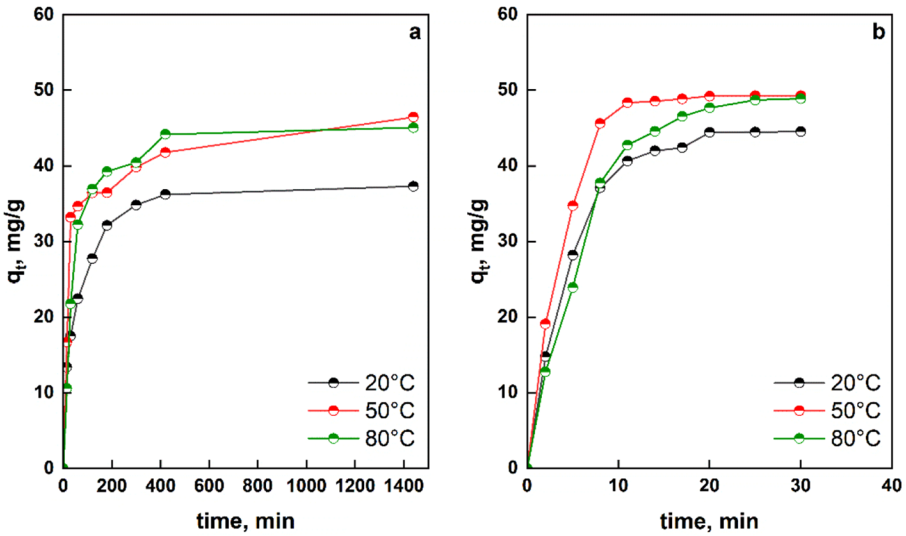

Fig. 5 q_t versus time (at different temperatures) for the adsorption of MB at **a** pH = 3 and **b** pH = 12

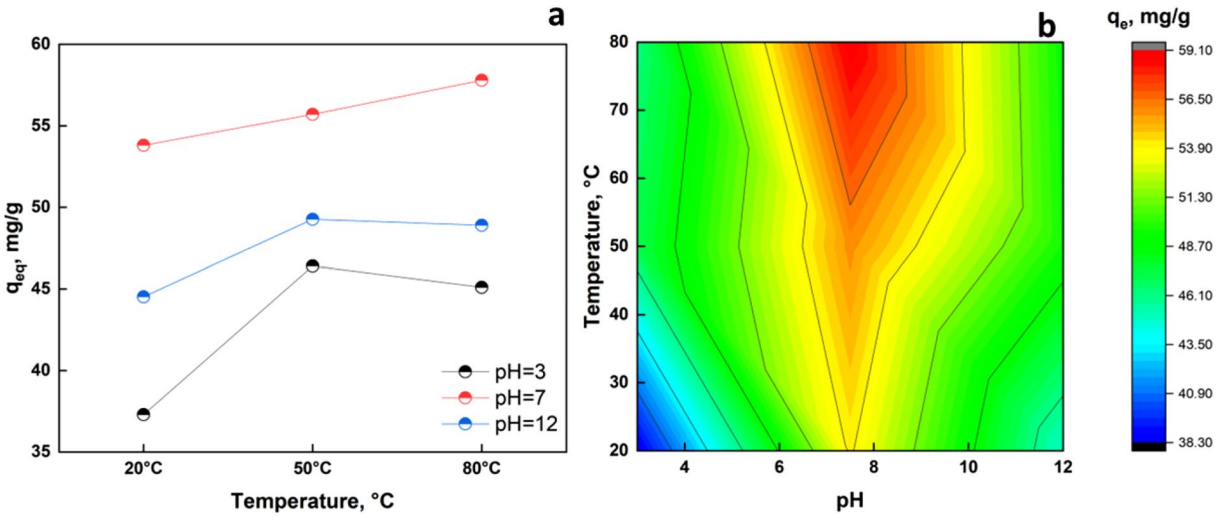

Fig. 7 Effects of pH and T on the equilibrium adsorption capacity: **a** scatter data and **b** a 2D contour plot

Table 2 Empirical mathematical models of k_2, q_e and t/q_t as functions of the pH at different temperatures

$T = 20$ °C	$k_2 = -0.004 + 0.00188 \times \mathrm{pH} - 0.000105 \times \mathrm{pH}^2$
	$q_e = 12 + 10.55 \times \mathrm{pH} - 0.65 \times \mathrm{pH}^2$
	$\frac{t}{q_t} = \frac{1}{(-0.004 + 0.00188 \times \mathrm{pH} - 0.000105 \times \mathrm{pH}^2) \times (12 + 10.55 \times \mathrm{pH} - 0.65 \times \mathrm{pH}^2)^2} + \frac{t}{12 + 10.55 \times \mathrm{pH} - 0.65 \times \mathrm{pH}^2}$
$T = 50$ °C	$k_2 = -0.0032 + 0.00244 \times \mathrm{pH} - 0.00022 \times \mathrm{pH}^2$
	$q_e = 32 + 6.13 \times \mathrm{pH} - 0.39 \times \mathrm{pH}^2$
	$\frac{t}{q_t} = \frac{1}{(-0.0032+0.00244\times\mathrm{pH}-0.00022\times\mathrm{pH}^2)\times(32+6.13\times\mathrm{pH}-0.39\times\mathrm{pH}^2)^2} + \frac{t}{32+6.13\times\mathrm{pH}-0.39\times\mathrm{pH}^2}$
$T = 80$ °C	$k_2 = -0.006 + 0.0026 \times pH - 0.00016 \times pH^2$
	$q_e = 26 + 8.45 \times \mathrm{pH} - 0.54 \times \mathrm{pH}^2$
	$\frac{t}{q_t} = \frac{1}{(-0.006+0.0026\times\mathrm{pH}-0.00016\times\mathrm{pH}^2)\times(26+8.45\times\mathrm{pH}-0.54\times\mathrm{pH}^2)^2} + \frac{t}{26+8.45\times\mathrm{pH}-0.54\times\mathrm{pH}^2}$

discussed. However, at pH = 12, lower values of q_t were recorded respect to pH = 7 due to the potential demethylation of MB (Fa and Dk 2007).

As previously reported, fitting the adsorption data using the pseudo-second-order model allowed the values of k_2 and q_e to be calculated. Mathematical expressions were then used to modify the pseudo-second-order model by highlighting the effect of pH on the adsorption performance (Table 2).

These equations can then be used to derive the amount of MB adsorbed at any given initial pH, T and time.

Desorption studies and reusability

In order to fully study the adsorption performance and to evaluate the sustainability of the adsorption process, regeneration studies were carried out. Regeneration of the GO-modified HF adsorbent paves the way to affordable water remediation processes. The recovery (%) of the organic dye was evaluated as function of the number of adsorption tests (Fig. 8). It can be observed that there is a 15% drop in the adsorption performance after 30 regeneration cycles. The results show that the adsorbent could be continuously used for MB removal without noticeably affecting the adsorption performance.

Leaching

The GO can be released from the adsorbent through leaching, causing secondary pollution, which could be hard to control (Malhotra et al. 2020). Figure 9 reports the GO leaching (µg/L) as a function of adsorption time (h).

It appears that after 240 h, only 0.15 µg/L of GO was leached, making it possible to still guarantee high adsorption capacity despite the leached GO. So, the GO/HF can

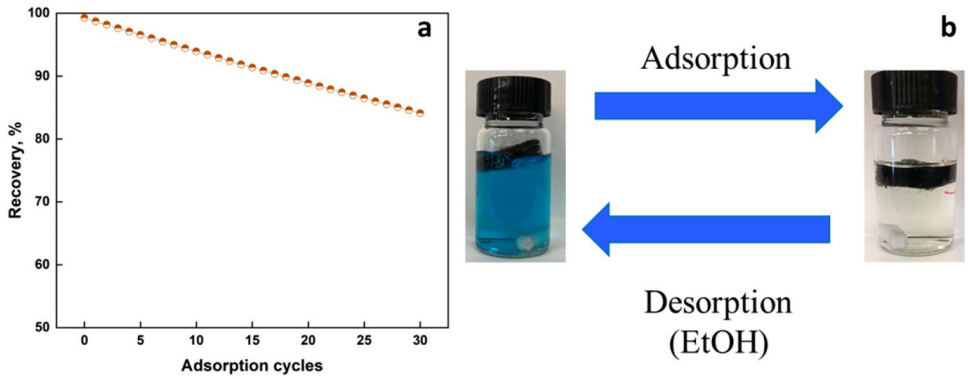

Fig. 8 **a** Recovery (%) as a function of the number of adsorption cycles and **b** photographs of the MB solution before and after adsorption

be used, recovered, and reused without any noticeable loss of performance. This finding could be associated with the covalent binding of GO to the OS-modified HF.

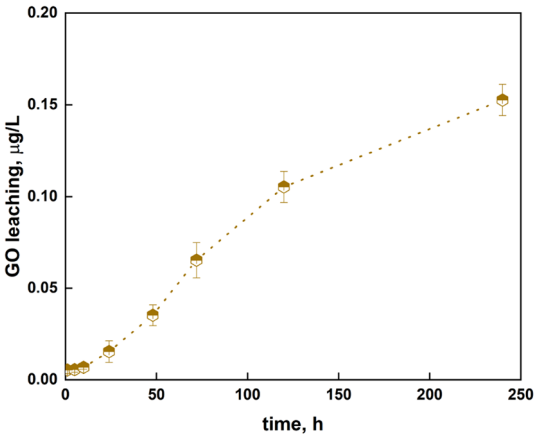

Fig. 9 GO leaching as a function of time (h)

Adsorption mechanism

The adsorption mechanism can provide more insight into the phenomena involved in the adsorption process. Considering the collected data, this paper proposes a potential adsorption mechanism based on (i) electrostatic interactions, (ii) hydrogen bonding, (iii) π–π interactions and (iv) van der Waals forces (Fig. 10).

The dye adsorption could occur due to the electrostatic forces between the cationic MB ions and negatively charged OH and COO^- groups on the basal planes and edges of GO sheets. Also, π–π coupling could exist between the C=C of MB and delocalized π electrons in the benzene rings. It follows that the presence of GO contributes to increasing the density of epoxide, hydroxyl and carboxyl groups, leading to the generation of strong electrostatic interactions and π–π electron coupling. The sorption of methylene blue could occur due to the ability of the MB to form micelles (monomeric or dimeric) in aqueous solution. So, the following possible mechanism could be considered (Ofomaja 2008):

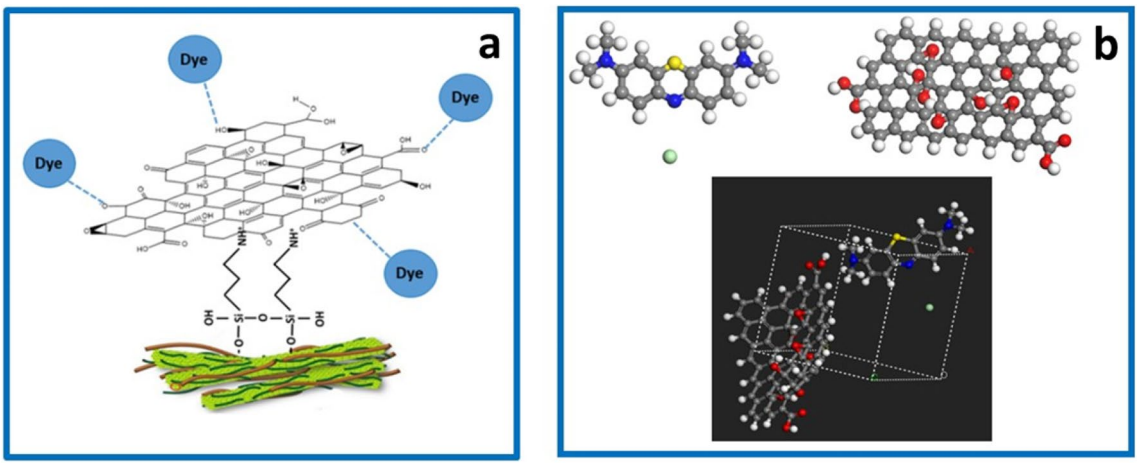

Fig. 10 **a** Adsorption mechanism of MB on GO/HF and **b** molecular modeling of the GO–MB interaction

Table 3 Comparison of the adsorption capacities (q_t) of natural adsorbents for MB removal

Adsorbent	q_t, mg/g	Reference
Magnetite geopolymer composite	76.34	Al-husseiny and Ebrahim (2022)
Konjac glucomannan-based magnetic carbon aerogels	9.37	Ye et al. (2016)
Fallen leaf biochar	101.27	Ji et al. (2019)
Luffa cylindrica fibers	49	Demir et al. (2008)
Biochar from seaweed	512.67	Ahmed et al. (2019)
Raspberry leaves	244.6	Mosoarca et al. (2022)
Fruit-peel-derived activated carbon	142.86	Gupta et al. (2022)
Turmeric/PVA/CMC	6.27	Radoor et al. (2022)
Moroccan clay	456.62	Loutfi et al. (2023)
Silica-coated soy waste	90	Batool and Valiyaveettil (2021)
Pseudo-stem banana fibers	42.28	Rahman et al. (2022)
Fly-ash-based spheres	79.7	Novais et al. (2019)
Papaya bark fibers	66.67	Nipa et al. (2023)
Cellulose-chitosan beads	55	Al-Ghamdi (2022)
Typha latifolia	54.73	El Amri et al. (2022)
Activated carbon/zeolite	51	Mohamed et al. (2022)
Chitosan lignin membrane	241.62	Vedula and Yadav (2022)

$$MB^{+} + GO - HF^{-} \leftrightarrow MB(GO - HF)$$

$$MB_2^{2+} + 2GO - HF^{-} \leftrightarrow MB_2(GO - HF)_2 + 2\,H^{+}$$

The interaction of MB with GO was proven through computational analysis. The geometrically optimized structures of GO and MB as well as the amorphous cell containing the studied compounds are reported in Fig. 10b. The analysis proved that the total energy of the system is 546.88 kcal/mol, the van der Waals energy is 38.13 kcal/mol, while the electrostatic energy is – 371.77 kcal/mol.

Comparison with other natural adsorbents

Table 3 reports the adsorption capacities of some natural adsorbents. The adsorption capacity of the designed GO/HF adsorbent was comparable to those of other bioadsorbents (Santoso et al. 2020), suggesting that it is a promising green adsorbent for wastewater remediation.

Concluding remarks

The production of environmentally friendly sorbents is considered one of the most promising techniques in water remediation. This manuscript focused on the use of hemp fibers, the least valuable part of the *Cannabis sativa* plant, as a support for producing a green adsorbent based on carbon-modified HF. A novel adsorbent for methylene blue removal from wastewaters was fabricated and characterized. The adsorbent was tested in batch conditions. The effects of the pH regime and temperature were correlated to the adsorption performance. The adsorption process appeared to be dependent on the pH and slightly affected by the temperature. The pH level greatly affects the adsorption process since electrostatic interactions can be generated between cationic MB molecules and electron-rich groups on the surface. The adsorption capacity at $T = 20$ °C changed from 37 to 54 mg/g upon increasing the pH from 3 to 7.5, while it decreased to 44.5 mg/g upon further increasing the pH to 12, due to the demethylation of MB. Also, when $T = 80$ °C, q_t is 45.1, 57.8 and 48.9 mg/g at pH = 3, 7.5 and 12, respectively, proving the endothermic behavior of the process. Moreover, MB adsorption follows the pseudo-second-order model, proving that the adsorption process involves chemisorption: there is a surface complexation reaction between the MB and the negative charges present on the modified HF. The produced adsorbent is chemically stable, showing no noticeable leaching of GO over time. Reusability studies showed that q_t reduced by about 15% after 30 cycles. The presented data proved that hemp fibers modified with GO could potentially be used as novel and cheaper adsorbent materials in wastewater treatment processes. A low amount of the designed adsorbent is able to completely decolorize an aqueous solution of methylene blue within a short time. This research paves the way for the application of a novel bioadsorbent based on the use of an agro-waste resource. A further experimental campaign will aim to investigate the mineralization and the degradation of the adsorbent as the process conditions change. Also, a study of the economic

aspects of the adsorbent is mandatory to facilitate the successful use of the material in water depollution and reuse processes.

Funding Open access funding provided by Università degli Studi di Salerno within the CRUI-CARE Agreement.

Data availability The data that used in this study is available on reasonable request.

References

Abbaz A, Arris S, Viscusi G et al (2023) Adsorption of Safranin O dye by alginate/pomegranate peels beads: kinetic, isotherm and thermodynamic studies. Gels 9:916. https://doi.org/10.3390/GELS9110916

Agarwal UP, Reiner RS, Ralph SA (2010) Cellulose I crystallinity determination using FT-Raman spectroscopy: univariate and multivariate methods. Cellulose 17:721–733. https://doi.org/10.1007/s10570-010-9420-z

Ahmad MA, Ahmad N, Bello OS (2015) Adsorption kinetic studies for the removal of synthetic dye using durian seed activated carbon. J Dispers Sci Technol 36:670–684. https://doi.org/10.1080/01932691.2014.913983

Ahmed MJ, Okoye PU, Hummadi EH, Hameed BH (2019) High-performance porous biochar from the pyrolysis of natural and renewable seaweed (*Gelidiella acerosa*) and its application for the adsorption of methylene blue. Bioresour Technol 278:159–164. https://doi.org/10.1016/J.BIORTECH.2019.01.054

Al-Ghamdi YO (2022) Immobilization of cellulose extracted from *Robinia Pseudoacacia* seed fibers onto chitosan: chemical characterization and study of methylene blue removal. Arab J Chem 15:104066. https://doi.org/10.1016/J.ARABJC.2022.104066

Al-husseiny RA, Ebrahim SE (2022) Effective removal of methylene blue from wastewater using magnetite/geopolymer composite: synthesis, characterization and column adsorption study. Inorg Chem Commun 139:109318. https://doi.org/10.1016/J.INOCHE.2022.109318

Ali NS, Jabbar NM, Alardhi SM et al (2017) Adsorption of methyl violet dye onto a prepared bio-adsorbent from date seeds: isotherm, kinetics, and thermodynamic studies. Heliyon. https://doi.org/10.1016/j.heliyon.2022.e10276

Allahbakhsh A, Noei Khodabadi F, Hosseini FS, Haghighi AH (2017) 3-Aminopropyl-triethoxysilane-functionalized rice husk and rice husk ash reinforced polyamide 6/graphene oxide sustainable nanocomposites. Eur Polym J 94:417–430. https://doi.org/10.1016/j.eurpolymj.2017.07.031

Al-Musawi TJ, Arghavan SMA, Allahyari E et al (2023) Adsorption of malachite green dye onto almond peel waste: a study focusing on application of the ANN approach for optimization of the effect of environmental parameters. Biomass Convers Biorefin 13:12073–12084. https://doi.org/10.1007/S13399-021-02174-6/FIGURES/8

Al-Rawi UA, Sher F, Hazafa A et al (2020) Catalytic activity of Pt loaded zeolites for hydroisomerization of n-hexane using supercritical CO_2. Ind Eng Chem Res 59:22092–22106. https://doi.org/10.1021/ACS.IECR.0C05184

Al-Rawi UA, Sher F, Hazafa A et al (2021) Synthesis of Zeolite supported bimetallic catalyst and application in n-hexane hydroisomerization using supercritical CO_2. J Environ Chem Eng 9:105206. https://doi.org/10.1016/J.JECE.2021.105206

Batool A, Valiyaveettil S (2021) Chemical transformation of soya waste into stable adsorbent for enhanced removal of methylene blue and neutral red from water. J Environ Chem Eng 9:104902. https://doi.org/10.1016/J.JECE.2020.104902

Bingol D, Tekin N, Alkan M (2010) Brilliant Yellow dye adsorption onto sepiolite using a full factorial design. Appl Clay Sci 50:315–321. https://doi.org/10.1016/j.clay.2010.08.015

Chong KY, Chia CH, Chook SW et al (2018) Simplified production of graphene oxide assisted by high shear exfoliation of graphite with controlled oxidation. New J Chem 42:4507–4512. https://doi.org/10.1039/c7nj04911k

Crini G, Torri G, Lichtfouse E et al (2019) Dye removal by biosorption using cross-linked chitosan-based hydrogels. Environ Chem Lett 17:1645–1666

Demir H, Top A, Balköse D, Ülkü S (2008) Dye adsorption behavior of *Luffa cylindrica* fibers. J Hazard Mater 153:389–394. https://doi.org/10.1016/J.JHAZMAT.2007.08.070

Eddy NO, Garg R, Garg R et al (2023) Waste to resource recovery: mesoporous adsorbent from orange peel for the removal of trypan blue dye from aqueous solution. Biomass Convers Biorefin 13:13493–13511. https://doi.org/10.1007/S13399-022-02571-5/FIGURES/9

El Amri A, Bensalah J, Idrissi A et al (2022) Adsorption of a cationic dye (Methylene bleu) by *Typha latifolia*: equilibrium, kinetic, thermodynamic and DFT calculations. Chem Data Coll 38:100834. https://doi.org/10.1016/J.CDC.2022.100834

Fa B, Dk S (2007) Simulation of dye adsorption by beech sawdust as affected by pH. J Hazard Mater 141:668–679. https://doi.org/10.1016/J.JHAZMAT.2006.07.033

Faridi AW, Imran M, Tariq GH et al (2023) Synthesis and characterization of high-efficiency halide perovskite nanomaterials for light-absorbing applications. Ind Eng Chem Res 62:4494–4502. https://doi.org/10.1021/ACS.IECR.2C00416/ASSET/IMAGES/LARGE/IE2C00416_0011.JPEG

Faruk O, Bledzki AK, Fink HP, Sain M (2012) Biocomposites reinforced with natural fibers: 2000–2010. Prog Polym Sci 37:1552–1596

Feng Y, Yang F, Wang Y et al (2011) Basic dye adsorption onto an agro-based waste material—Sesame hull (*Sesamum indicum* L.). Bioresour Technol 102:10280–10285. https://doi.org/10.1016/J.BIORTECH.2011.08.090

Forgacs E, Cserháti T, Oros G (2004) Removal of synthetic dyes from wastewaters: a review. Environ Int 30:953–971

Futalan CM, Choi AES, Soriano HGO et al (2022) Modification strategies of kapok fiber composites and its application in the adsorption of heavy metal ions and dyes from aqueous solutions: a systematic review. Int J Environ Res Public Health 19:2703. https://doi.org/10.3390/IJERPH19052703

Garg N, Deep A, Sharma AL (2023) Performance evaluation of agro-waste (sugarcane bagasse ash) for MB dye effluents removal under UV and dark environmental conditions: a cost-effective

approach. Clean Technol Environ Policy 25:1973–1987. https://doi.org/10.1007/S10098-023-02484-5/FIGURES/9
Gupta K, Khatri OP (2017) Reduced graphene oxide as an effective adsorbent for removal of malachite green dye: Plausible adsorption pathways. J Colloid Interface Sci 501:11–21. https://doi.org/10.1016/J.JCIS.2017.04.035
Gupta SA, Vishesh Y, Sarvshrestha N et al (2022) Adsorption isotherm studies of Methylene blue using activated carbon of waste fruit peel as an adsorbent. Mater Today Proc 57:1500–1508. https://doi.org/10.1016/J.MATPR.2021.12.044
Hao OJ, Kim H, Chiang PC (2000) Decolorization of wastewater. Crit Rev Environ Sci Technol 30:449–505
Hashem A, Aniagor CO, Morsy OM et al (2022) Apricot seed shell: an agro-waste biosorbent for acid blue193 dye adsorption. Biomass Convers Biorefin 1:1–14. https://doi.org/10.1007/S13399-022-03272-9/TABLES/7
Ho YS, McKay G (1998) Sorption of dye from aqueous solution by peat. Chem Eng J 70:115–124. https://doi.org/10.1016/s0923-0467(98)00076-1
Javed SI, Hussain Z (2015) Covalently functionalized graphene oxide—characterization and its electrochemical performance. Int J Electrochem Sci 10:9475–9487
Jeong HK, Lee YP, Jin MH et al (2009) Thermal stability of graphite oxide. Chem Phys Lett 470:255–258. https://doi.org/10.1016/j.cplett.2009.01.050
Ji B, Wang J, Song H, Chen W (2019) Removal of methylene blue from aqueous solutions using biochar derived from a fallen leaf by slow pyrolysis: behavior and mechanism. J Environ Chem Eng 7:103036. https://doi.org/10.1016/J.JECE.2019.103036
Kale RD, Potdar T, Gorade V (2019) Treatment of C.I. reactive blue-21 effluent by microcrystalline cellulose grafted with APTES: Kinetics, isotherm and thermodynamic study. Sustain Environ Res. https://doi.org/10.1186/s42834-019-0007-6
Kargarzadeh H, Ahmad I, Abdullah I et al (2012) Effects of hydrolysis conditions on the morphology, crystallinity, and thermal stability of cellulose nanocrystals extracted from kenaf bast fibers. Cellulose 19:855–866. https://doi.org/10.1007/s10570-012-9684-6
Kargarzadeh H, Sheltami RM, Ahmad I et al (2015) Cellulose nanocrystal: a promising toughening agent for unsaturated polyester nanocomposite. Polymer (Guildf) 56:346–357. https://doi.org/10.1016/j.polymer.2014.11.054
Kavitha D, Namasivayam C (2007) Experimental and kinetic studies on methylene blue adsorption by coir pith carbon. Bioresour Technol 98:14–21. https://doi.org/10.1016/j.biortech.2005.12.008
Khaniabadi YO, Heydari R, Nourmoradi H et al (2016) Low-cost sorbent for the removal of aniline and methyl orange from liquid-phase: Aloe Vera leaves wastes. J Taiwan Inst Chem Eng 68:90–98. https://doi.org/10.1016/J.JTICE.2016.09.025
Khanjanzadeh H, Behrooz R, Bahramifar N et al (2018) Surface chemical functionalization of cellulose nanocrystals by 3-aminopropyltriethoxysilane. Int J Biol Macromol 106:1288–1296. https://doi.org/10.1016/j.ijbiomac.2017.08.136
Kong D, Wilson LD (2020) Uptake of methylene blue from aqueous solution by pectin-chitosan binary composites. J Compos Sci 4:95. https://doi.org/10.3390/jcs4030095
Konicki W, Aleksandrzak M, Mijowska E (2017) Equilibrium, kinetic and thermodynamic studies on adsorption of cationic dyes from aqueous solutions using graphene oxide. Chem Eng Res Des 123:35–49. https://doi.org/10.1016/J.CHERD.2017.03.036
Kuang Y, Zhang X, Zhou S (2020) Adsorption of methylene blue in water onto activated carbon by surfactant modification. Water (Basel) 12:587. https://doi.org/10.3390/w12020587
Largitte L, Pasquier R (2016) A review of the kinetics adsorption models and their application to the adsorption of lead by an activated carbon. Chem Eng Res Des 109:495–504. https://doi.org/10.1016/j.cherd.2016.02.006
Li Y, Du Q, Liu T et al (2013) Comparative study of methylene blue dye adsorption onto activated carbon, graphene oxide, and carbon nanotubes. Chem Eng Res Des 91:361–368. https://doi.org/10.1016/J.CHERD.2012.07.007
Li J, Cui J, Yang J et al (2016) Silanized graphene oxide reinforced organofunctional silane composite coatings for corrosion protection. Prog Org Coat 99:443–451. https://doi.org/10.1016/j.porgcoat.2016.07.008
Li H, Liu L, Cui J et al (2020) High-efficiency adsorption and regeneration of methylene blue and aniline onto activated carbon from waste edible fungus residue and its possible mechanism. RSC Adv 10:14262–14273. https://doi.org/10.1039/d0ra01245a
Liu M, Thygesen A, Summerscales J, Meyer AS (2017) Targeted pretreatment of hemp bast fibres for optimal performance in biocomposite materials: a review. Ind Crops Prod 108:660–683
Lorenc-Grabowska E, Gryglewicz G (2007) Adsorption characteristics of Congo Red on coal-based mesoporous activated carbon. Dyes Pigm 74:34–40. https://doi.org/10.1016/j.dyepig.2006.01.027
Loryuenyong V, Totepvimarn K, Eimburanapravat P et al (2013) Preparation and characterization of reduced graphene oxide sheets via water-based exfoliation and reduction methods. Adv Mater Sci Eng. https://doi.org/10.1155/2013/923403
Loutfi M, Mariouch R, Mariouch I et al (2023) Adsorption of methylene blue dye from aqueous solutions onto natural clay: equilibrium and kinetic studies. Mater Today Proc 72:3638–3643. https://doi.org/10.1016/J.MATPR.2022.08.412
Ma X, Zhao S, Tian Z et al (2022) MOFs meet wood: reusable magnetic hydrophilic composites toward efficient water treatment with super-high dye adsorption capacity at high dye concentration. Chem Eng J 446:136851. https://doi.org/10.1016/J.CEJ.2022.136851
Maleki S, Karimi-Jashni A (2020) Optimization of Ni(II) adsorption onto Cloisite Na+ clay using response surface methodology. Chemosphere 246:125710. https://doi.org/10.1016/j.chemosphere.2019.125710
Malhotra N, Villaflores OB, Audira G et al (2020) Toxicity studies on graphene-based nanomaterials in aquatic organisms: current understanding. Molecules 25:3618. https://doi.org/10.3390/MOLECULES25163618
Mohamed F, Shaban M, Zaki SK et al (2022) Activated carbon derived from sugarcane and modified with natural zeolite for efficient adsorption of methylene blue dye: experimentally and theoretically approaches. Sci Rep 12:1–18. https://doi.org/10.1038/s41598-022-22421-8
Mohammad N, Atassi Y (2020) Adsorption of methylene blue onto electrospun nanofibrous membranes of polylactic acid and polyacrylonitrile coated with chloride doped polyaniline. Sci Rep. https://doi.org/10.1038/s41598-020-69825-y
Mohammadi N, Khani H, Gupta VK et al (2011) Adsorption process of methyl orange dye onto mesoporous carbon material—kinetic and thermodynamic studies. J Colloid Interface Sci 362:457–462. https://doi.org/10.1016/J.JCIS.2011.06.067
Mohyudin S, Farooq R, Jubeen F et al (2022) Microbial fuel cells a state-of-the-art technology for wastewater treatment and bioelectricity generation. Environ Res 204:112387. https://doi.org/10.1016/J.ENVRES.2021.112387
Molla A, Youk JH (2022) Chemical clock reactions with organic dyes: Perspective, progress, and applications. Dyes Pigm 202:110237. https://doi.org/10.1016/J.DYEPIG.2022.110237
Morin-Crini N, Loiacono S, Placet V et al (2018) Hemp-based materials for metal removal. Springer, Cham, pp 1–34
Mosoarca G, Popa S, Vancea C et al (2022) Removal of methylene blue from aqueous solutions using a new natural lignocellulosic adsorbent—raspberry (*Rubus idaeus*) leaves powder. Polymers (Basel) 14:1966. https://doi.org/10.3390/POLYM14101966/S1

Nipa ST, Shefa NR, Parvin S et al (2023) Adsorption of methylene blue on papaya bark fiber: Equilibrium, isotherm and kinetic perspectives. Results Eng 17:100857. https://doi.org/10.1016/J.RINENG.2022.100857

Novais RM, Carvalheiras J, Tobaldi DM et al (2019) Synthesis of porous biomass fly ash-based geopolymer spheres for efficient removal of methylene blue from wastewaters. J Clean Prod 207:350–362. https://doi.org/10.1016/J.JCLEPRO.2018.09.265

Ofomaja AE (2008) Sorptive removal of Methylene blue from aqueous solution using palm kernel fibre: Effect of fibre dose. Biochem Eng J 40:8–18. https://doi.org/10.1016/J.BEJ.2007.11.028

Oladipo AA, Ifebajo AO (2018) Highly efficient magnetic chicken bone biochar for removal of tetracycline and fluorescent dye from wastewater: two-stage adsorber analysis. J Environ Manag 209:9–16. https://doi.org/10.1016/j.jenvman.2017.12.030

Ouedrhiri A, Ait Himi M, Youbi B et al (2022) Biochar material derived from natural waste with superior dye adsorption performance. Mater Today Proc 66:259–267. https://doi.org/10.1016/J.MATPR.2022.04.928

Phuong DTM, Loc NX (2022) Rice straw biochar and magnetic rice straw biochar for Safranin O adsorption from aqueous solution. Water (Switzerland) 14:186. https://doi.org/10.3390/W14020186/S1

Qu T, Yao X, Owens G et al (2022) A sustainable natural clam shell derived photocatalyst for the effective adsorption and photodegradation of organic dyes. Sci Rep 12:1–14. https://doi.org/10.1038/s41598-022-06981-3

Rachini A, Le Troedec M, Peyratout C, Smith A (2009) Comparison of the thermal degradation of natural, alkali-treated and silane-treated hemp fibers under air and an inert atmosphere. J Appl Polym Sci 112:226–234. https://doi.org/10.1002/app.29412

Radoor S, Karayil J, Jayakumar A et al (2022) Ecofriendly and low-cost bio adsorbent for efficient removal of methylene blue from aqueous solution. Sci Rep 12:1–20. https://doi.org/10.1038/s41598-022-22936-0

Rahman MW, Nipa ST, Rima SZ et al (2022) Pseudo-stem banana fiber as a potential low-cost adsorbent to remove methylene blue from synthetic wastewater. Appl Water Sci 12:1–16. https://doi.org/10.1007/S13201-022-01769-2/TABLES/5

Raji M, Mekhzoum MEM, el Qaiss AK, Bouhfid R (2016) Nanoclay modification and functionalization for nanocomposites development: effect on the structural, morphological, mechanical and rheological properties. Springer, Singapore, pp 1–34

Rasheed S, Sher F, Rasheed T et al (2021) Hydrothermally engineered Ni–CuC hybrid nanocomposites: Structural and morphological investigations with potential fuel catalytic applications. Mater Chem Phys 270:124837. https://doi.org/10.1016/J.MATCHEMPHYS.2021.124837

Rashtbari Y, Sher F, Afshin S et al (2022) Green synthesis of zero-valent iron nanoparticles and loading effect on activated carbon for furfural adsorption. Chemosphere 287:132114. https://doi.org/10.1016/J.CHEMOSPHERE.2021.132114

Robles E, Urruzola I, Labidi J, Serrano L (2015) Surface-modified nano-cellulose as reinforcement in poly(lactic acid) to conform new composites. Ind Crops Prod 71:44–53. https://doi.org/10.1016/j.indcrop.2015.03.075

Rosli NA, Ahmad MA, Noh TU (2023) Unleashing the potential of pineapple peel-based activated carbon: Response surface methodology optimization and regeneration for methylene blue and methyl red dyes adsorption. Inorg Chem Commun 155:111041. https://doi.org/10.1016/J.INOCHE.2023.111041

Sağlam S, Türk FN, Arslanoğlu H (2023) Use and applications of metal-organic frameworks (MOF) in dye adsorption: Review. J Environ Chem Eng 11:110568. https://doi.org/10.1016/J.JECE.2023.110568

Sajab MS, Chia CH, Zakaria S et al (2011) Citric acid modified kenaf core fibres for removal of methylene blue from aqueous solution. Bioresour Technol 102:7237–7243. https://doi.org/10.1016/J.BIORTECH.2011.05.011

Sanjay MR, Siengchin S, Parameswaranpillai J et al (2019) A comprehensive review of techniques for natural fibers as reinforcement in composites: preparation, processing and characterization. Carbohydr Polym 207:108–121

Santoso E, Ediati R, Kusumawati Y et al (2020) Review on recent advances of carbon based adsorbent for methylene blue removal from waste water. Mater Today Chem 16:100233. https://doi.org/10.1016/J.MTCHEM.2019.100233

Sawpan MA, Pickering KL, Fernyhough A (2011) Effect of various chemical treatments on the fibre structure and tensile properties of industrial hemp fibres. Compos Part A Appl Sci Manuf 42:888–895. https://doi.org/10.1016/j.compositesa.2011.03.008

Sehar S, Sher F, Zhang S et al (2020) Thermodynamic and kinetic study of synthesised graphene oxide-CuO nanocomposites: a way forward to fuel additive and photocatalytic potentials. J Mol Liq 313:113494. https://doi.org/10.1016/J.MOLLIQ.2020.113494

Serodre T, Oliveira NAP, Miquita DR et al (2019) Surface silanization of graphene oxide under mild reaction conditions. J Braz Chem Soc 30:2488–2499. https://doi.org/10.21577/0103-5053.20190167

Shaiful Sajab M, Hua Chia C, Zakaria S, et al (2011) Citric acid modified kenaf core fibres for removal of methylene blue from aqueous solution. Bioresour Technol 102:7237–7243. https://doi.org/10.1016/j.biortech.2011.05.011

Sher F, Iqbal SZ, Rasheed T et al (2021) Coupling of electrocoagulation and powder activated carbon for the treatment of sustainable wastewater. Environ Sci Pollut Res 28:48505–48516. https://doi.org/10.1007/S11356-021-14129-5/FIGURES/11

Shi Y, Chang Q, Zhang T et al (2022) A review on selective dye adsorption by different mechanisms. J Environ Chem Eng 10:108639. https://doi.org/10.1016/J.JECE.2022.108639

Shirmardi M, Mahvi AH, Hashemzadeh B et al (2013) The adsorption of malachite green (MG) as a cationic dye onto functionalized multi walled carbon nanotubes. Korean J Chem Eng 30:1603–1608. https://doi.org/10.1007/S11814-013-0080-1/METRICS

Slatni I, Dhiffalah A, Elberrichi FZ et al (2022) Investigation of adsorption properties of modified DD kaolins to microporous material type 13X zeolite in treatment of textile industry effluent: experiments and theoretical approach. Euro-Mediterr J Environ Integr 7:415–432. https://doi.org/10.1007/S41207-022-00324-4/FIGURES/14

Smječanin N, Bužo D, Mašić E et al (2022) Algae based green biocomposites for uranium removal from wastewater: kinetic, equilibrium and thermodynamic studies. Mater Chem Phys 283:125998. https://doi.org/10.1016/J.MATCHEMPHYS.2022.125998

Szabó T, Berkesi O, Dékány I (2005) DRIFT study of deuterium-exchanged graphite oxide. Carbon N Y 43:3186–3189. https://doi.org/10.1016/j.carbon.2005.07.013

Terpáková E, Kidalová L, Eštoková A, et al (2012) Chemical modification of hemp shives and their characterization. Procedia Eng 42:931–941

Thong Z, Gao J, Lim JXZ et al (2018) Fabrication of loose outer-selective nanofiltration (NF) polyethersulfone (PES) hollow fibers via single-step spinning process for dye removal. Sep Purif Technol 192:483–490. https://doi.org/10.1016/j.seppur.2017.10.031

Tkaczyk A, Mitrowska K, Posyniak A (2020) Synthetic organic dyes as contaminants of the aquatic environment and their implications for ecosystems: a review. Sci Total Environ 717:137222. https://doi.org/10.1016/J.SCITOTENV.2020.137222

Varghese AG, Paul SA, Latha MS (2019) Remediation of heavy metals and dyes from wastewater using cellulose-based adsorbents. Environ Chem Lett 17:867–877

Vedula SS, Yadav GD (2022) Wastewater treatment containing methylene blue dye as pollutant using adsorption by chitosan lignin membrane: Development of membrane, characterization and kinetics of adsorption. J Indian Chem Soc 99:100263. https://doi.org/10.1016/J.JICS.2021.100263

Vimonses V, Lei S, Jin B et al (2009) Kinetic study and equilibrium isotherm analysis of Congo Red adsorption by clay materials. Chem Eng J 148:354–364. https://doi.org/10.1016/j.cej.2008.09.009

Viscusi G, Gorrasi G (2021) A novel approach to design sustainable fiber reinforced materials from renewable sources: mathematical modeling for the evaluation of the effect of fiber content on biocomposite properties. J Mark Res 12:717–726. https://doi.org/10.1016/j.jmrt.2021.03.017

Viscusi G, Barra G, Gorrasi G (2020) Modification of hemp fibers through alkaline attack assisted by mechanical milling: effect of processing time on the morphology of the system. Cellulose 27:8653–8665. https://doi.org/10.1007/s10570-020-03406-0

Viscusi G, Lamberti E, Gorrasi G (2021a) Hemp fibers modified with graphite oxide as green and efficient solution for water remediation: application to methylene blue. Chemosphere. https://doi.org/10.1016/J.CHEMOSPHERE.2021.132614

Viscusi G, Lamberti E, Gorrasi G (2021b) Design of sodium alginate/soybean extract beads loaded with hemp hurd and halloysite as novel and sustainable systems for methylene blue adsorption. Polym Eng Sci. https://doi.org/10.1002/PEN.25839

Viscusi G, Pantani R, Gorrasi G (2021d) Transport properties of water vapor through hemp fibers modified with a sustainable process: effect of surface morphology on the thermodynamic and kinetic phenomena. Appl Surf Sci 541:148433. https://doi.org/10.1016/j.apsusc.2020.148433

Viscusi G, Lamberti E, Gorrasi G (2022) Design of a hybrid bio-adsorbent based on Sodium Alginate/Halloysite/Hemp hurd for methylene blue dye removal: kinetic studies and mathematical modeling. Colloids Surf A Physicochem Eng Asp 633:127925. https://doi.org/10.1016/J.COLSURFA.2021.127925

Wang Z, Hu C, Tu D et al (2020) Preparation and adsorption property of activated carbon made from *Camellia olerea* shells. J for Eng 5:96–102. https://doi.org/10.13360/J.ISSN.2096-1359.202001032

Widiartyasari Prihatdini R, Suratman A, Siswanta D (2023) Linear and nonlinear modeling of kinetics and isotherm of malachite green dye adsorption to trimellitic-modified pineapple peel. Mater Today Proc 88:33–40. https://doi.org/10.1016/J.MATPR.2023.07.108

Yan S, Yang Y, Song L et al (2017) Influence of 3-aminopropyltriethoxysilane-graphite oxide composite on thermal stability and mechanical property of polyethersulfone. High Perform Polym 29:960–975. https://doi.org/10.1177/0954008316665679

Yang L, Shang J, Dou B et al (2022) CO_2-responsive functional cotton fibers decorated with Ag nanoparticles for "smart" selective and enhanced dye adsorption. J Hazard Mater 429:128327. https://doi.org/10.1016/J.JHAZMAT.2022.128327

Ye S, Jin W, Huang Q et al (2016) KGM-based magnetic carbon aerogels matrix for the uptake of methylene blue and methyl orange. Int J Biol Macromol 92:1169–1174. https://doi.org/10.1016/J.IJBIOMAC.2016.07.106

Yin C, Qiu S, Zhang S et al (2020) Strength degradation mechanism of iron coke prepared by mixed coal and Fe_2O_3. J Anal Appl Pyrolysis 150:104897. https://doi.org/10.1016/J.JAAP.2020.104897

Zafar N, Niazi MBK, Sher F et al (2021) Starch and polyvinyl alcohol encapsulated biodegradable nanocomposites for environment friendly slow release of urea fertilizer. Chem Eng J Adv 7:100123. https://doi.org/10.1016/J.CEJA.2021.100123

Zhang L, Zeng Y, Cheng Z (2016) Removal of heavy metal ions using chitosan and modified chitosan: a review. J Mol Liq 214:175–191

Zhou C, Wu Q, Lei T, Negulescu II (2014) Adsorption kinetic and equilibrium studies for methylene blue dye by partially hydrolyzed polyacrylamide/cellulose nanocrystal nanocomposite hydrogels. Chem Eng J 251:17–24. https://doi.org/10.1016/j.cej.2014.04.034

Authors and Affiliations

Gianluca Viscusi[1] · Francesco Napolitano[1] · Giuliana Gorrasi[1]

✉ Gianluca Viscusi
gviscusi@unisa.it

[1] Department of Industrial Engineering, University of Salerno, Via Giovanni Paolo II, 132, 84084 Fisciano, Salerno, Italy